Received: 16 March 2022 | Accepted: 9 June 2022

DOI: 10.1002/jcc.26957

RESEARCH ARTICLE

Journal of COMPUTATIONAL CHEMISTRY WILEY

Molecular properties and tautomeric equilibria of isolated flavins

Felipe Curtolo | **Guilherme M. Arantes**

Department of Biochemistry, Instituto de Química, Universidade de São Paulo, São Paulo, SP, Brazil

Correspondence
Felipe Curtolo and Guilherme M. Arantes, Department of Biochemistry, Instituto de Química, Universidade de São Paulo, Av. Prof. Lineu Prestes 748, 05508-900, São Paulo, SP, Brazil.
Email: felipe.curtolo@usp.br and garantes@iq.usp.br

Funding information
Fundação de Amparo à Pesquisa do Estado de São Paulo, Grant/Award Numbers: 2017/26109-0, 2019/21856-7

Abstract

Flavins are employed as redox cofactors and chromophores in a plethora of flavoenzymes. Their versatility is an outcome of intrinsic molecular properties of the isoalloxazine ring modulated by the protein scaffold and surrounding solvent. Thus, an investigation of isolated flavins with high-level electronic-structure methods and with error assessment of the calculated properties will contribute to building better models of flavin reactivity. Here, we benchmarked ground-state properties such as electron affinity, gas-phase basicity, dipole moment, torsion energy, and tautomer stability for lumiflavins in all biologically relevant oxidation and charge states. Overall, multiconfigurational effects are small and chemical accuracy is achieved by coupled-cluster treatments of energetic properties. Augmented basis sets and extrapolations to the complete basis-set limit are necessary for consistent agreement with experimental energetics. Among DFT functionals tested, M06-2X shows the best performance for most properties, except gas-phase basicity, in which M06 and CAM-B3LYP perform better. Moreover, dipole moments of radical flavins show large deviations for all functionals studied. Tautomers with noncanonical protonation states are significantly populated at normal temperatures, adding to the complexity of modeling flavins. These results will guide future computational studies of flavoproteins and flavin chemistry by indicating the limitations of electronic-structure methodologies and the contributions of multiple tautomeric states.

KEYWORDS
electronic-structure, flavoprotein, isoalloxazine, quantum chemistry, tautomerism

1 | INTRODUCTION

Flavins are prosthetic groups composed by the fused tricyclic ring isoalloxazine (benzo[g]pteridine, Figure 1). All natural flavins are methylated at carbons C7 and C8, but the group bound to nitrogen N10 varies.[1] Riboflavin, or vitamin B_2, has a ribityl group bound to N10, while its photoproduct, lumiflavin, has a methyl bound to N10.[2] The ubiquitous coenzymes flavin mononucleotide (FMN) and flavin adenine dinucleotide (FAD) have ribityl phosphate and ribityl-adenosine diphosphate moieties respectively attached to N10.

Proteins equipped with flavins, known as flavoproteins, are involved in a wide range of catalytic and signaling processes.[2,3]

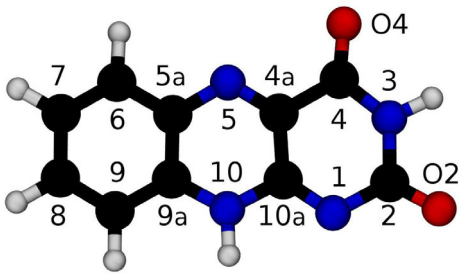

FIGURE 1 Structure and heavy-atom numbering for the isoalloxazine ring, the core group of flavins responsible for their redox and photophysical properties

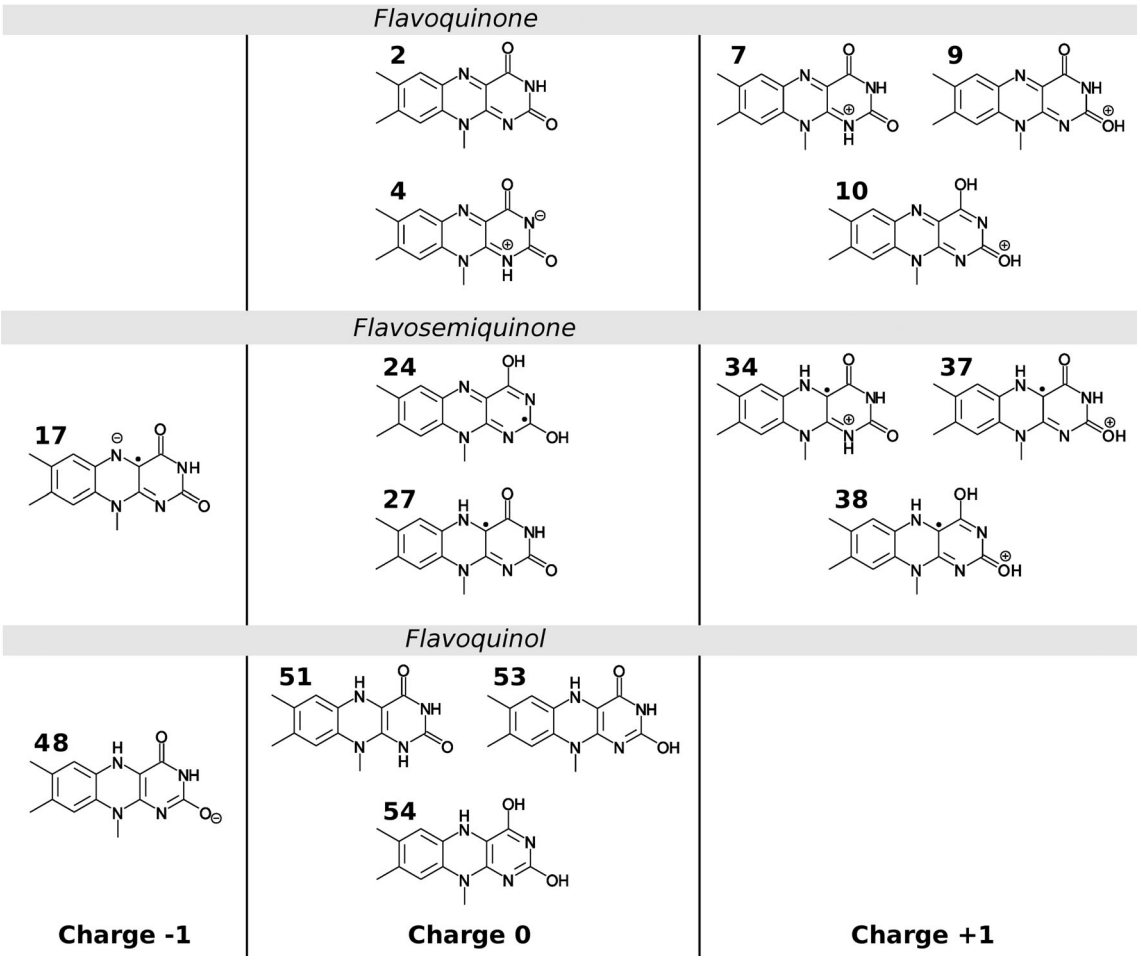

FIGURE 2 Structural formula of the main lumiflavin tautomers discussed here with their respective numbering, redox and charge state

Redox flavoproteins participate in single-electron transfer reactions,[4] in oxygen-dependent oxidation,[5] and in proton-coupled electron transfers (PCET) with varying number of electrons.[2,6,7] Flavin chromophores are found in blue-light protein receptors[3] and in photodependent enzymes.[8] Recently, the biological role of flavins as general acid–base catalysts has also been demonstrated.[9,10]

This versatility of flavoprotein function results from their ability to assume different redox, protonation and electronic states. Flavins are found in fully oxidized flavoquinone, 1-electron reduced flavosemiquinone radical, and two-electron reduced flavoquinol forms (Figure 2).[1] Charge states with anionic, neutral, zwitterionic or cationic character are also possible, with their relative stability depending on the microenvironment and protein scaffold.[2,11]

An additional layer of variability concerns flavin tautomerism.[12–18] N3, N5, and N1 are canonical protonation sites and are often found protonated in flavoproteins under neutral pH.[1] However, alternative tautomers with protonations in O2 and O4 were already observed.[9,18,19] In flavosemiquinones, spin delocalization allows even carbons $C4_a$ and $C10_a$ as possible protonation sites.[16]

Computational methods have been used to study flavins for more than four decades.[20–23] While early works were based on semiempirical models, the first ab initio and density functional theory (DFT) studies of flavins were performed in the late 1990s[12–15] followed by a number of computational investigations (Table S1).[16–18,24–56] The vast majority were based on DFT for ground-state properties[14,16–18,24–36] or time-dependent DFT (TD-DFT) for excited-state calculations,[36–50] mostly focused on the neutral flavoquinone form using lumiflavin as a model system. High-level ab initio coupled-cluster EOM-CCSD[56] and approximate CC2[55] were used recently to calculate vertical ionization potentials and flavin excited states, respectively. Multireference CASPT2 calculations were also reported[51] and even relativistic contributions were obtained with 4-component TD-DFT.[54]

However, none of these studies addressed systematically the approximations employed in calculations for flavins of various forms. Here, we provide a benchmark evaluation for ground-state properties of isolated lumiflavin in all possible oxidation and protonation states (a total of 59 species, Figures S1, S2, and S3). After description of the computational methods, we first investigate the effects of static and dynamic electron correlation. The coupled-cluster level is found as an appropriate reference after validation in comparison to experimental structures, electron affinities, and gas-phase basicities. Then, we analyze in detail the performance of various electronic-structure methods, including a ladder DFT functionals, for the calculation of

molecular-structural, energetic, electrical, and chemical properties. We note that alternative protonation sites may be intrinsically stabilized and challenge the canonical assignment of tautomeric equilibria in flavins.

2 | COMPUTATIONAL METHODS

2.1 | Geometry optimization

All flavins studied here had their geometry optimized with the B3LYP functional[57,58] and def2-TZVP[59] basis set. Optimizations of closed-shell flavins were performed with restricted Kohn-Sham formalism and flavosemiquinones with an open shell were optimized with unrestricted calculations. Spin contamination in the latter was small and the average deviation from the expected value $\langle S^2 \rangle$ was 0.013, with the largest being 0.023 for **36**. All calculations were conducted with ORCA 4.1.1,[60,61] using tight SCF convergence criteria and increased integration grids. All optimized structures (lumiflavins **1**–**59**) are available online.[62]

The DFT accuracy in geometry optimizations (Section 3.2) was evaluated for functionals BLYP,[63,64] PBE,[65] M06-L,[66] PBE0,[67] and M06-2X.[68] Among ab initio wave-function methods, coupled cluster CCSD(T) with the domain-based local-pair natural orbital (DLPNO) approximation[69] and the augmented basis set aug-cc-pVTZ[70] was used to optimize the geometry of the isoalloxazine ring in comparison to DFT and experimental geometries. The aug-cc-pVTZ/C[71] auxiliary basis set was employed, with tight DLPNO thresholds. Also, the DLPNO-CCSD(T) geometry optimization was considered converged when root-mean-square gradient was less than 0.0015 $E_h.a_0^{-1}$ and the maximum component of the gradient was less than 0.0050 $E_h.a$. This looser convergence criteria had to be employed here due to the computational demands of the method.

Flavins can bend when N5 and N10 move above the isoalloxazine ring plane (Figure 3). This "butterfly" motion is observed mainly in flavoquinols and is relevant for flavin reactivity and dynamics. The associated torsion energy E_{tor} varies with the flavin redox and protonation state. Here, E_{tor} is defined as the difference in electronic potential energy between flavin in its planar and bent optimized conformations.

Geometries with isoalloxazine ring torsion were generated by constrained optimizations with B3LYP/def2-TZVP. The dihedral angles between atoms C4–N5–N10–C9 and N1–N10–N5–C6 (Figure 1) were restrained. Stable geometries for flavoquinols show both dihedrals close to 150° (Figure 3). In flavoquinones and flavosemiquinones, these dihedrals were constrained to 150.0° to generate bent conformations, and in flavoquinols they were constrained to 180.0° to obtain planar geometries.

2.2 | Model chemistry

Wave-function single-reference calculations with the MP2, CCSD, and CCSD(T) methods[72] employed Dunning's correlation-consistent

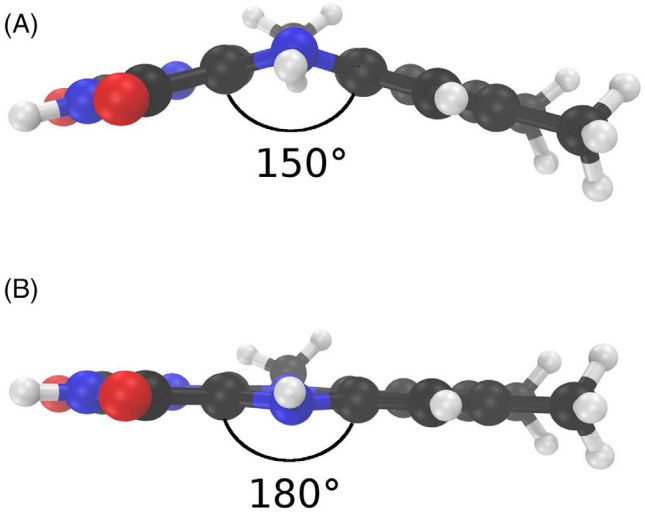

FIGURE 3 Planarity of the isoalloxazine ring. (A) Bent conformation found in stable reduced flavoquinol and (B) planar conformation found in stable oxidized flavoquinone

basis-set families, cc-pV*n*Z[73] and aug-cc-pV*n*Z,[70] with n = D,T,Q. The frozen-core approximation was employed in all post-Hartree-Fock calculations. To avoid spin contamination in flavosemiquinones, restricted open-shell Hartree-Fock was used as the zeroth-order reference wave function. DLPNO-CCSD and DLPNO-CCSD (T) approximations[69] were also tested. For flavosemiquinones, unrestricted Hartree-Fock was performed first, and quasi-restricted orbitals were generated prior to the coupled-cluster excitations. This is the default approach employed by ORCA. The DLPNO approximation required the use of auxiliary cc-pV*n*Z/C or aug-cc-pV*n*Z/C[71] basis sets. Tight DLPNO thresholds ("TightPNO" keyword in ORCA) were employed.[74]

Multiconfigurational wave functions (CASSCF)[72] were built with all isoalloxazine π orbitals in the active space, that is, a CAS(14,14) for flavoquinones or a CAS(15,14) for flavosemiquinones. The initial set of molecular orbitals were MP2 natural orbitals and the composition of the active space was checked before and after convergence. The contribution of dynamical correlation was calculated with the partially contracted version of NEVPT2.[75] The frozen-core approximation was employed with all electrons occupying internal orbitals 1 s removed from the perturbation treatment.

For DFT calculations, the minimally augmented version of Karlsruhe def2 basis-set family,[59] ma-TZVP,[76] was employed. This basis set is efficient and accurate in DFT calculations. The usage of an augmented version is due to the presence of anionic flavins.

Seventeen functionals were tested: BLYP,[63,64] OLYP,[64,77] PBE,[65] BPBE,[63,65] OPBE,[65,77] TPSS,[78] M06-L,[66] B3LYP,[57,58] B3LYP + D3,[79,80] PBE0,[67] O3LYP,[81] M06,[68] M06-2X,[68] CAM-B3LYP,[82] LC-BLYP,[83] ωB97X,[84] and B2PLYP.[85]

The resolution of identity (RI) was employed with auxiliary basis def2/J[86] to approximate the Coulomb integrals. For hybrid functionals, chain-of-spheres approximations (COSX)[87,88] was also used in the calculation of the Hartree-Fock exchange. For

flavosemiquinones, unrestricted Kohn-Sham was used. All calculations were performed with tight SCF convergence criteria and increased integration grids.

Zero-point vibrational energies (*ZPV E*) were calculated for stationary geometries at the B3LYP/def2-TZVP level without empirical scaling factors. Entropic and enthalpic contributions were calculated at 298.15 K using the quasi rigid-rotor-harmonic-oscillator approximation (QRRHO).[89,90] No imaginary frequencies were observed for all optimized flavins, indicating they were true minima.

The conductor-like polarizable continuum model (CPCM)[91] was used as an implicit-solvent model. Water solvation was mimicked with a dielectric constant and a refractive index set to 80.4 and 1.33, respectively. Nevertheless, we refrain from extensively including environmental effects and calculating condensed-phase properties here. These effects represent additional modeling difficulties, which may be tackled in future studies.

2.3 | Basis-set extrapolation

Wave-function calculations are particularly sensitive to basis-set incompleteness. Thus, the complete basis-set limit (CBS) was approximated by two-point extrapolations. For single-point energies, the mean-field SCF energy $E_{\mathrm{SCF}}{}^{\mathrm{CBS}}$ and the correlation energy $E_{\mathrm{corr}}{}^{\mathrm{CBS}}$ are extrapolated separately, following Equations (1)[92] and (2),[93,94] respectively. Electric dipole moments $\boldsymbol{\mu}^{\mathrm{CBS}}$ are extrapolated using Equation (3)[95]:

$$E_{\mathrm{SCF}}^{(X)} = E_{\mathrm{SCF}}^{\mathrm{CBS}} + Ae^{-\alpha\sqrt{X}}, \tag{1}$$

$$E_{\mathrm{corr}}^{\mathrm{CBS}} = \frac{X^{\beta}E_{\mathrm{corr}}^{(X)} - Y^{\beta}E_{\mathrm{corr}}^{(Y)}}{X^{\beta} - Y^{\beta}}, \tag{2}$$

$$|\boldsymbol{\mu}|^{\mathrm{CBS}} = \frac{X^3|\boldsymbol{\mu}|^{(X)} - Y^3|\boldsymbol{\mu}|^{(Y)}}{X^3 - Y^3}, \tag{3}$$

where X and Y are the basis-set cardinal numbers: 2 for double-zeta (D), 3 for triple-zeta (T) and 4 for quadruple-zeta (Q) extrapolations. For cc-pV[D/T]Z, $\alpha = 4.42$ and $\beta = 2.46$; for aug-cc-pV[D/T]Z, $\alpha = 4.30$ and $\beta = 2.51$ and for aug-cc-pV[T/Q]Z, $\alpha = 5.79$ and $\beta = 3.05$.[96] In Equation (1), A is a constant determined by the two-point extrapolation.

2.4 | Molecular properties

The electric dipole moment ($\boldsymbol{\mu}$), a first-order electrical property, was obtained from DFT calculations directly from the SCF solution. For MP2 and B2PLYP methods, the relaxed electron density was calculated to account for orbital relaxation effects. For the calculation of dipole moments with DLPNO-CCSD, the parameter T_{CutPNO} was tightened to 10^{-8} because the use of DLPNO default truncation parameters would lead to inaccurate values.[97] All dipoles were calculated at equilibrium geometries, and the dipole origin was set to the center of mass.

The electron affinity (*EA*) of a molecule is defined as the negative of the energy difference of ground vibrational/rotational states before (M) and after ($M^{\bullet-}$) electron attachment. This process may induce a geometry change in the molecule. Electron affinities obtained from the energy difference of equilibrium geometries and associated *ZPV E* contributions are called adiabatic (EA_{adiab}):

$$EA_{\mathrm{adiab}} = (E_{\mathrm{M}} + ZPVE_{\mathrm{M}}) - (E_{\mathrm{M}^{\bullet-}} + ZPVE_{\mathrm{M}^{\bullet-}}), \tag{4}$$

where E_{M} and $E_{\mathrm{M}^{\bullet-}}$ are single-point energies for optimized geometries of the oxidized and reduced species. However, experimental measurements probe a different, thermalized condition and often consider *EA* (here called EA_{therm}) as the negative of the enthalpy of the reaction $\mathrm{M} + \mathrm{e}^- \rightleftharpoons \mathrm{M}^{\bullet-}$[34,98]:

$$EA_{\mathrm{therm}} = H_{\mathrm{M}} + H_{\mathrm{e}^-} - H_{\mathrm{M}^{\bullet-}} \tag{5}$$

where H is the enthalpy of formation and $H_{\mathrm{e}^-} \equiv 0$.[98] Here, EA_{therm} was calculated by including enthalpic contributions obtained with the QRRHO approximation at the B3LYP/def2-TZVP level.

The gas-phase basicity (*GB*) of a molecule M at temperature T is the negative of the Gibbs free energy for the protonation reaction $\mathrm{M} + \mathrm{H}^+ \rightleftharpoons \mathrm{MH}^+$. Flavins have multiple protonation sites and the calculated *GB* was determined by using a population-weighted average (Equation (6)) with each tautomer MH_i^+ having a weight w_i given by its canonical probability (Equation (7)).[99] For example, if M is **2**, then $\mathrm{MH}^+ = \{$**7**, **9**, **12**, **13**$\}$, and the *GB* of M is an average over contributions from this set of flavins:

$$GB(T) = -\sum_i w_i \left[G\left(\mathrm{MH}_i^+\right) - G(\mathrm{M}) - G\left(\mathrm{H}^+\right)\right], \tag{6}$$

$$w_i = \frac{e^{-\Delta G_i/k_B T}}{\sum_i e^{-\Delta G_i/k_B T}}, \tag{7}$$

where k_B is the Boltzmann constant and ΔG_i the relative free energy between tautomer MH_i^+ and the tautomer with the lowest free energy.

To calculate *GB* with different model chemistries, entropic and enthalpic contributions were obtained with B3LYP/def2-TZVP except for the electronic contribution, which was replaced by the energy calculated with the method of choice. The Gibbs free energy of the proton was considered to be −0.010 E_h, the free energy of a monoatomic ideal gas at 298.15 K.

3 | RESULTS AND DISCUSSION

3.1 | Electron correlation and reference model chemistry

Static electron correlation is important for the description of flavins in excited states,[51] but it is unclear whether it also plays a role in

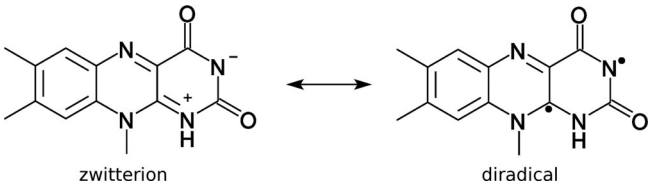

FIGURE 4 Resonance structures of **4**. When N1 (see Figure 1 for atom-numbering) is protonated, zwitterion or diradical (note unpaired electrons in $C10_a$ and N3) resonance structures are possible

ground-state properties. We first applied the τ_1 diagnostics[100] to all flavins studied here (Tables S2, S3, and S4) and checked that they show τ_1 values smaller than 0.020, indicating negligible static correlation. The only borderline case was **17** in bent conformation with τ_1 of 0.020 (Table S3) and discussed in more detail below.

Multiconfigurational calculations in selected flavosemiquinones and zwitterionic flavoquinones were conducted. The unpaired electron in the former may delocalize over the π-conjugated system, while the latter have competing resonance structures (Figure 4), possibly amounting for sizable multiconfigurational effects.

In Table 1, it is shown for semiquinones **17**, **27**, and **37** that the total energy difference between single-reference MP2 and multireference NEVPT2 is less than 1 mE_h, even for the bent **17** which displayed the borderline τ_1 value mentioned above, indicating that static correlation is not important. The correlation energy recovered in CASSCF is mainly dynamic correlation obtained by the full-CI treatment within the active space. The main electronic configuration in the CASSCF wave function for the three planar flavosemiquinones has a weight of 0.81 while all other configurations have weights less than 0.02. This configuration has only one single-occupied molecular orbital (MO), spatially delocalized over the isoalloxazine ring. The same configuration is observed in the Hartree-Fock wave function, and thus the effect of spin delocalization is properly accounted with the mean-field treatment.

For zwitterionic **4**, a state-average (SA) CASSCF calculation with two roots (50:50 weights) was performed to account for both resonance structures (Figure 4). Analysis of the obtained localized orbitals shows that the first (R1) and second (R2) roots correspond respectively to zwitterionic and diradical states. For natural orbitals, the principal configuration of root R1 contributes with 78% of the total CI expansion, while all remaining configurations have weights lower than 2%. For the root R2, the two principal configurations contribute with 48% and 20% of the total CI expansion. This is an indication of multiconfigurational character for the excited diradical state. It suggests that appropriate multiconfigurational methods should be used to calculate properties and reactivity which may involve flavin diradical states.

In Table 2, it is shown that the NEVPT2 energy for R1 is 3 mE_h smaller than the single-reference MP2 solution with a zwitterionic resonance structure. Thus, the multiconfigurational contribution for the ground-state R1 is small and the energetics is described well by a single-reference method.

Additionally, the energy difference found between the two roots for **4** (R1 and R2, 0.11 E_h with NEVPT2 in Table 2) exemplify that excited electronic states in flavins have considerably high energies and their nonadiabatic crossings may be safely neglected for calculation of ground-state properties.

In the condensed phase, however, dielectric and specific contacts may stabilize zwitterionic flavins and increase the importance of their resonance states and the associated multiconfigurational character. For instance, although the MP2/cc-pVDZ energy for the isolated neutral tautomer **2** is 54 mE_h lower than **4**, solvation in a polar dielectric (estimated by the CPCM model for water)[91,101] stabilizes preferentially the zwitterion and the energy difference drops to 29 mE_h, still in favor of the neutral **2**. Yet, specific interactions in enzymes may stabilize N1 protonation (Figure 2), shifting even further this energy difference and the associated tautomeric equilibria (**2** $\rightleftharpoons$ **4**).

Results shown above indicate that a single-reference electronic-structure method should be sufficient for the description of ground-state properties and reactions of flavins studied here. Dynamic electron correlation should also be recovered. Applying the gold-standard single-reference CCSD(T) method to flavins is only computationally feasible using a double-zeta basis set, which compromises the amount of correlation recovered. Thus, we first compared the full CCSD(T) within this limited basis set and the DLPNO local-pair approximation,[69] which provides linear scaling with system size and allows coupled-cluster calculations of flavins with a larger basis.

In Table 3, both CCSD(T) and DLPNO-CCSD(T) calculations employed quasi-restricted orbitals. The error due to the DLPNO approximation is significant in the triples correction for two representative flavins and reaches 11 mE_h for **17** even using tight calculation thresholds (TightPNO keyword). This error is much higher than often observed in smaller molecules[74] and similar to deviations found for transition metal complexes.[102] For the flavins, the error may be attributed to the delocalized and resonant nature of the electron distribution in the tricyclic isoalloxazine ring. Nevertheless, the error in relative energies due to the DLPNO approximation decreases to 1.3 mE_h, as in the reaction **2** $\rightleftharpoons$ **17** $+ e^-$. This is the expected upper limit in the accuracy of relative energies for flavin reactions obtained here from DLPNO-CCSD(T) calculations with larger (triple-zeta and extrapolated) basis sets. Nevertheless, the DLPNO-CCSD(T) method was chosen here as the reference model chemistry.

3.2 | Accuracy of calculated molecular structure, dipole, and torsion energy

The calculated equilibrium geometry of isoalloxazine ring may be assessed by comparison with solid-state crystallography of related flavins. The structure for 3-methyl-lumiflavin has been determined by X-ray diffraction[103] and Table 4 shows a comparison of bond lengths with the gas-phase optimized geometry of isoalloxazine. The uncertainty in bond lengths of the crystal structure is 0.003 Å, so there is no significant difference between calculated and experimental bond lengths for C=C, C=N, and C=O. The difference of 0.014 and

TABLE 1 Electronic energy (in E_h) obtained for **17**, **27**, and **37** with the cc-pVDZ basis set

Method	17	17(bent)	27	37
HF	−866.938886	−866.929755	−867.484272	−867.881032
CASSCF[a]	−867.082975	−867.073693	−867.635744	−868.026266
MP2	−869.654678	−869.644219	−870.196964	−870.595394
NEVPT2[a]	−869.653852	−869.645101	−870.197265	−870.595219

[a]The active space (15 e^- in 14 MO) contains the complete resonant π-system.

TABLE 2 Electronic energy (in E_h) obtained for zwitterionic **4** with the cc-pVDZ basis set

Method	Total energy
SA-CASSCF R1[a]	−866.993155
SA-CASSCF R2[b]	−866.908477
NEVPT2 R1	−869.562887
NEVPT2 R2	−869.449373
MP2	−869.559812

[a]First root with zwitterionic character.
[b]Second root with diradical character.

TABLE 3 Electron correlation energies (E_{Method}–E_{HF}, in E_h) for **2** and the reduced flavosemiquinone **17**

Method	2	17
CCSD/cc-pVDZ	−2.772852	−2.796138
DLPNO-CCSD/cc-pVDZ	−2.772857	−2.793963
CCSD(T)/cc-pVDZ	−2.893783	−2.916723
DLPNO-CCSD(T)/cc-pVDZ	−2.883622	−2.905234

TABLE 4 Average lengths (in Å) for different bond types in isoalloxazine ring

Bond	Experiment[a]	Calculated[b]	Δ
C=C	1.396	1.398	0.002
C=N	1.302	1.298	0.004
C=O	1.213	1.212	0.001
C–N	1.375	1.383	0.008
C–C	1.465	1.479	0.014

[a]3-methyl-lumiflavin crystal structure.[103].
[b]DLPNO-CCSD(T)/aug-cc-pVTZ geometry for isoalloxazine.

0.008 Å observed for the more flexible C–C and C–N bonds may be attributed to packing effects in the crystal environment, which may shorten the bond lengths. In conclusion, the similarity between calculated and experimental bond lengths corroborates that DLPNO-CCSD(T)/aug-cc-pVTZ provides accurate geometries.

Table 5 shows mean unsigned errors (MUE) and maximum absolute errors (MAX) in bond lengths and angles for selected DFT functionals tested in comparison to reference geometries optimized at the DLPNO-CCSD(T)/aug-cc-pVTZ level for the isoalloxazine molecule (Figure 1). B3LYP gives the smallest errors regarding bond lengths

TABLE 6 DLPNO-CCSD(T)/aug-cc-pVTZ energy (in E_h) for **2** and **17** with geometries optimized by different DFT functionals

Functional	E_2	E_{17}	ΔE
PBE	−870.70018	−870.76169	0.06151
M06-L	−870.69987	−870.76142	0.06155
B3LYP	−870.70076	−870.76216	0.06140

TABLE 5 Mean unsigned errors (MUE) and maximum absolute errors (MAX) of isoalloxazine bond lengths and angles obtained from DFT optimizations

	Length (Å)		Angle (°)	
Functional	MUE	MAX	MUE	MAX
BLYP	0.009	0.020	0.32	1.12
PBE	0.007	0.016	0.27	0.78
M06-L	0.005	0.012	0.32	0.93
B3LYP	0.003	0.0103	0.35	1.38
PBE0	0.006	0.014	0.29	1.08
M06-2X	0.006	0.016	0.45	1.64

Note: Reference values comes from DLPNO-CCSD(T)/aug-cc-pVTZ geometry.

(both MUE and MAX), while PBE gives the smallest errors in bond angles.

Table 6 shows total energies obtained with DLPNO-CCSD(T)/aug-cc-pVTZ after optimization of **2** and **17** with functionals PBE, M06-L, and B3LYP. The smallest energies for both flavins are found for the B3LYP geometry, indicating a better performance. But, differences between relative energies ΔE are negligible (<0.15 mE_h) suggesting that optimizations with any of these three functionals would result in geometries with equivalent quality.

It is unlikely that B3LYP performance is an artifact of error cancellation because of the favorable comparison to DLPNO-CCSD(T)/aug-cc-pVTZ geometries (Table 5). Thus, the B3LYP/def2-TZVP model was chosen for geometry optimizations of all equilibrium and bent structures studied here.

For flavoquinols **40**, **41**, and **56**, that show protonations in both N1 and O2/N3, pirimidalization of N10 is more pronounced than in the other flavoquinols, and their methyl group remains completely below the isoalloxazine ring. This change in methyl position make N10 more negative, which stabilizes electrostatically the adjacent positive

TABLE 7 Magnitude of μ (in D) calculated for **2** with different methods

	MP2	DLPNO-CCSD
aug-cc-pVDZ	8.97	8.96
aug-cc-pVTZ	9.01	9.02
aug-cc-pV[D/T]Z	9.03	9.04

sites {N1, O2, N3} that are bound to two or three protons in **40**, **41**, and **56**.

Flavins may undergo a butterfly motion bending the isoalloxazine ring (Figure 3). When fully reduced, electronic repulsions favor the pirimidalization of N5 and N10, and lead to ring bending.[24] Thus, it is relevant to check the associated torsion energy (E_{tor}) for which DLPNO-CCSD(T)/aug-cc-pV[D/T]Z was used as reference.

It was suggested experimentally for several flavoquinol derivatives in solution that E_{tor} is lower than 20 kJ.mol^{-1}.[104] For isolated flavoquinols calculated here, E_{tor} has a similar magnitude (Table S19). For flavoquinones and flavosemiquinones, experimental data show that these flavins assume planar or quasi-planar conformations,[18,24,103] again in agreement with results here.

The electric dipole moment μ was evaluated here because this property is relevant to flavin interactions in condensed phase. Its calculation by coupled-cluster methods is very demanding, so the accuracy of μ obtained with MP2 was assessed first (Table 7). Regardless of the basis set used, MP2 and DLPNO-CCSD dipoles differ on their magnitudes by only 0.01 D for **2** and MP2/aug-cc-pV[D/T]Z dipoles were chosen as a reference here.

3.3 | Comparison with experimental gas-phase reactions

Experimental electron affinity and gas-phase basicity are available for **2**[34] and are used here for comparison with various levels of theory and basis set. Tables 8 and S5 show an opposed trend for EA_{therm} increasing with the basis-set size while *GB* decreases, particularly in the DLPNO-CCSD(T) level.

Employing augmented basis sets is essential for a correct description of the diffuse anionic product (**17**). For instance, the cc-pVTZ set gives less accurate *EA* than aug-cc-pVDZ for all methods tested. Augmented sets also give a better description for the *GB* calculation. MP2 calculations employing any CBS extrapolation provides results in agreement with both experimental properties within their uncertainties, probably due to fortuitous error cancellation. For more reliable coupled-cluster methods, the DLPNO-CCSD(T) level with the aug-cc-pVQZ set or with the extrapolated CBS limit (either [T/Q]Z or [D/T]Z) provide excellent results.

It should also be noted that EA_{adiab} is systematically smaller than EA_{therm} for all calculation levels (Table S6). The latter was used for comparisons here because it is a better approximation to *EA* measured experimentally in thermalized conditions. However, it is unclear which

TABLE 8 Electron affinity (*EA*, in eV) and gas-phase basicity (*GB*, in kJ.mol^{-1}) for **2**

Method	EA_{therm}	*GB*
MP2		
cc-pV[D/T]Z	1.88	926
aug-cc-pV[D/T]Z	1.93	923
aug-cc-pV[T/Q]Z	1.94	924
DLPNO-CCSD		
cc-pV[D/T]Z	1.77	938
aug-cc-pV[D/T]Z	1.81	935
aug-cc-pV[T/Q]Z	1.80	932
DLPNO-CCSD(T)		
cc-pVDZ	1.21	950
cc-pVTZ	1.59	940
cc-pV[D/T]Z	1.78	934
aug-cc-pVDZ	1.75	925
aug-cc-pVTZ	1.79	929
aug-cc-pVQZ	1.80	928
aug-cc-pV[D/T]Z	1.82	930
aug-cc-pV[T/Q]Z	1.81	928
Experimental[34]	1.86 ± 0.12	919 ± 9

temperature the *GB* experiments were conducted at.[34] Here $T = 298.15$ K is assumed, but this may be an additional source of uncertainty for our calculated values in relation to the experiment.

By neglecting thermal and entropic contributions, *EA* and *GB* calculated with DLPNO-CCSD(T)/aug-cc-pV[T/Q]Z would yield 1.77 eV and 954 kJ.mol^{-1}, respectively. While *EA* would still agree with experiment within uncertainty, *GB* would disagree in 26 kJ.mol^{-1}. By also neglecting *ZPV E* corrections, *EA* and *GB* would become 1.69 eV and 988 kJ.mol^{-1}, largely degrading the calculated accuracy. Therefore, including zero-point vibrational (*ZPV E*) and thermal contributions is essential for quantitative agreement with experiment.

Due to the favorable comparisons shown in this section, reasonable computational cost and the more systematic behavior of coupled-cluster methods in recovering electron correlation, the DLPNO-CCSD(T)/aug-cc-pV[D/T]Z level was chosen here to produce reference energetic values for other flavin tautomers. Although other approximations are evoked here (harmonic vibrational modes, frozen-core energies, etc.), it may be concluded that electron and proton affinities for isolated flavins are well described with this level of theory and B3LYP/def2-TZVP geometry optimizations.

3.4 | Tautomer thermochemistry

As shown in Figure 2, flavins with given redox state and total charge may assume different tautomeric forms. For example, three tautomers (**6**, **7**, and **9**) are found for a cationic flavoquinone, by protonating two atoms in the set {N1, N3, O2}. Table 9 shows the calculated free

TABLE 9 Calculated[a] relative free energies (ΔG[298.15 K], in kJ.mol^{-1}) and equilibrium composition (in %) of isolated flavins with multiple tautomeric states

	ΔG	Composition
Flavoquinone neutral		
2	0.0	100.00
4	120.8	0.00
Flavoquinone cation		
7	11.2	1.07
9	0.0	98.82
10	17.0	0.11
Flavosemiquinone neutral		
24	13.2	0.48
27	0.0	99.52
Flavosemiquinone cation		
34	9.1	2.47
37	0.0	97.51
38	20.7	0.02
Flavoquinol neutral		
51	0.0	99.66
53	16.0	0.15
54	15.6	0.19

[a]DLPNO-CCSD(T)/aug-cc-pV[D/T]Z//B3LYP/def2-TZVP.

energy and equilibrium composition at 298.15 K for possible tautomers.

For flavoquinones, the most stable tautomers are **2** for neutral and **9** for cationic forms, in accordance with previous qualitative predictions.[12,14,18] However, the current results highlight that tautomers such as **10** are more stable than previously proposed. For instance, Dopfer et al.[18] obtained $\Delta G = 24.2$ kJ.mol^{-1} for **10** using B3LYP/cc-pVDZ calculations. Furthermore, Ridge et al.[34] performed B3LYP/6-31G* and M06-L/6-31G* calculations and suggested that **7** was more stable among the cationic forms. This disagreement with results reported here (Tables 9 and S7) may be caused by the geometry found by Ridge et al. after optimization which shows the dihedral N1–C2–O2–H rotated by 180° in comparison to the structures found here and previously.[18]

For flavosemiquinone, the most stable tautomer are **27** for neutral and **37** for cationic forms, again in qualitative agreement with previous calculations.[12,14,16] The relative energy of **34** was predicted to be 5.4 and 4.1 kJ.mol^{-1} higher than **37** by earlier calculations with HF/6-31G** and B3LYP/6-31G* methods, respectively.[12,14] These are potential energy values, but are similar to the free energy of 9.1 kJ.mol^{-1} reported here.

The work of Zheng and Ornstein[13] with HF/6-31G* calculations suggested that **27** was not the most stable neutral flavosemiquinone. Their conclusion disagrees qualitatively with the results shown here and in earlier publications.[14,16] We suspect that the approximate nature of the unrestricted HF calculation performed[13] lead to the wrong conclusion.

Hadad and Platz et al.[16] tested stabilities of alternative tautomers of neutral flavosemiquinones. They considered not only oxygens and nitrogens as possible protonation sites (See Figure S2), but also the carbons $C4_a$ and $C10_a$. Their B3LYP/6–31+G** calculations added by *ZPV E* agrees with ours and predict **27** as the most stable tautomer. Protonation at $C4_a$ and $C10_a$ resulted in tautomers 105.9 and 213.8 kJ.mol^{-1} more energetic than **27**, respectively.[16] This large energy difference indicates that flavin radicals with protonation at carbon will be unstable and irrelevant to tautomeric thermochemistry. Nevertheless, these species may still play a role as alternative reaction mechanisms and transient intermediates in flavoenzymes.

For flavoquinols, **51** is the most stable in the neutral form. Meyer et al. in an early study reported heats of formation calculated with the semiempirical method PM3 for different flavoquinol tautomers.[12] They found **51** as the most stable, **54** was 45.2 kJ.mol^{-1} more energetic and **53** was 25.9 kJ.mol^{-1} more energetic. These results disagree with the energies of 15.6 and 16.0 kJ.mol^{-1} reported here respectively, showing that the PM3 method (and possibly other semiempirical methods based in the NDDO approximation)[105] is inadequate to predict tautomeric equilibria of flavins.

Termochemical analysis at normal temperature may indicate if more than one tautomer can exist at equilibrium. For anionic flavins and neutral flavoquinone, there is a significantly lower energetic tautomer, comprising 100% of the ensemble: **17** is the tautomeric form adopted by anionic flavosemiquinone, **48** for anionic flavoquinol and **2** for neutral flavoquinone (See Tables S7, S8, and S9). In gas phase, only one tautomer needs to be accounted for when calculating thermodynamic properties for these molecules. Alternatively, cationic flavins, neutral flavosemiquinone, and neutral flavoquinol have more than one tautomer significantly populated (Table 9).

Only nitrogen sites (N1, N3, or N5) are protonated in the most stable tautomer of each redox and charge, except for the cationic flavins, **9** and **37**, which have O2 protonated. This unusual oxygen protonation is also found in **10, 24, 38, 53**, and **54**, which are within 20 kJ.mol^{-1} of the most stable tautomer in their respective redox and charge state. For instance, flavoquinol 51 has all three nitrogens protonated and the 54 tautomer, with O2 and O4 protonated, is 15.6 kJ.mol^{-1} more energetic. Other naturally occurring quinols such as ubiquinol and plastoquinol always have their oxygens protonated.[106,107] But the resonance structure in flavins results in stabilization of nitrogen protonation and (flavo)quinols without a phenol group.

The isolated *GB* of stable anionic flavosemiquinone **17** and stable anionic flavoquinol **48** are almost identical, 1336 and 1335 kJ.mol^{-1}, respectively (Tables S15 and S17). However, in aqueous solution, the flavosemiquinone is significantly more basic than the flavoquinol, with $pK_a \approx 8$ and 6, respectively for their conjugated acids.[1] For the stable neutral flavoquinone **2** and stable neutral flavosemiquinone **27**, although their $GB = 963$ and 930 kJ.mol^{-1}, respectively (Tables S14 and S16), their cationic conjugated acids in aqueous solution exist only under very low pH.[1]

TABLE 10 Mean unsigned errors (MUE) and maximum absolute errors (MAX) of properties calculated by DFT functionals for lumiflavin forms studied here

	EA_{adiab} (eV)		GB (kJ.mol^{-1})		$\|\|\mu\|\|$(D)		E_{tor} (kJ.mol^{-1})	
Functional	**MUE**	**MAX**	**MUE**	**MAX**	**MUE**	**MAX**	**MUE**	**MAX**
GGA and meta-GGA								
BLYP	0.30	0.74	13	34	0.47	1.45	3.3	6.2
OLYP	0.35	0.78	9	25	0.50	1.53	3.7	6.6
PBE	0.20	0.61	13	35	0.49	1.48	3.5	7.0
BPBE	0.22	0.65	9	25	0.50	1.48	3.5	7.0
OPBE	0.26	0.68	13	30	0.53	1.57	3.8	6.8
TPSS	0.25	0.65	8	19	0.50	1.49	3.0	6.7
M06-L	0.35	0.73	12	22	0.59	1.52	3.0	8.5
Hybrid								
B3LYP	0.22	0.53	5	14	0.48	1.32	2.3	7.2
B3LYP + D3	0.22	0.52	6	17	0.48	1.32	2.2	6.7
PBE0	0.22	0.44	5	13	0.49	1.33	2.3	7.9
O3LYP	0.21	0.56	6	21	0.46	1.36	3.1	8.1
M06	0.17	0.38	4	13	0.49	1.32	2.6	7.2
M06-2X	0.14	0.23	7	12	0.48	1.31	1.4	5.6
Range-separated								
CAM-B3LYP	0.22	0.31	4	12	0.53	1.25	2.1	7.0
LC-BLYP	0.20	0.33	22	32	0.54	1.27	2.0	6.6
ωB97X	0.23	0.37	7	15	0.55	1.34	1.5	6.1
Double-hybrid								
B2PLYP	0.17	0.38	8	18	0.44	1.43	1.6	5.0

Note: Reference values were obtained with DLPNO-CCSD(T) for energies and MP2 for dipoles, both with the aug-cc-pV[D/T]Z basis extrapolation.

This comparison reassert that the gas-phase basicity and electron affinity cannot be used directly as probes of condensed-phase basicity and redox potentials, as solvation modulates the ability to bind protons and electrons slightly differently for each flavin form. Nevertheless, the intrinsic tautomeric equilibria of isolated flavins described here builds the foundation for modeling their condensed-phase behavior by including the influence of microenvironments and light absorption as a perturbation of intrinsic equilibria.[12,14,17] For instance, the **9** ⇌ **7** equilibrium was suggested previously[12,14] and above (Section 3.1) to shift toward **7** formation in implicit solvent models. Explicit hydrogen bonds provided by flavoprotein scaffolds are expected to further affect flavin tautomerism.[11,33,108]

3.5 | Performance of DFT for molecular properties

As DFT is often employed for ground-state calculations of flavins, an appraisal of the performance of selected functionals in the computation of their molecular properties is useful and shown in Table 10. Properties for each flavin species and functional are shown in Tables S10–S19. MUE and MAX were calculated over different sets for each property. For EA_{adiab}, $N = 34$, comprising all flavoquinones and the neutral and cationic flavosemiquinones (**1**–**14** and **20**–**39**). Flavoquinols and anionic flavosemiquinone were removed as they would require calculation of unstable three-electron reduced species or generate unstable dianions, respectively. For *GB*, $N = 30$, comprising all anionic flavins, neutral flavoquinones, and flavosemiquinones (**1**–**5**, **15**–**19**, and **40**–**49**). Calculations of *GB* for neutral flavoquinols would result in high-energy four-time protonated flavins. For $\boldsymbol{\mu}$ and E_{tor}, N = 14, comprising the most stable tautomers in Figure 2 and excluding **4**.

The functional showing the lowest deviation varies with the calculated property. Overall, M06-2X shows the best performance, with the lowest MAX errors among GGA and hybrid functionals for all properties, and the lowest MUE for *EA* and E_{tor} properties among all functionals. Thus, M06-2X may be indicated for calculation of redox potentials of flavins. Surprisingly, this functional shows the highest MUE for *GB* among hybrid functionals. Alternatively, M06 and CAM-B3LYP perform particularly well for *GB* and dipole moments, so they may be indicated for the computation of tautomer thermochemistry in condensed phase, for instance using hybrid QC/MM potentials.[109,110] Among computationally cheaper GGA functionals, TPSS, BPBE, and pure PBE show the best overall performance. However, all GGA functionals except OPBE make qualitatively wrong predictions on the relative stability of flavosemiquinone tautomers.

The popular B3LYP functional performs well for all properties (maybe except for *EA*), while inclusion of D3 dispersion correction does not improve its accuracy. The higher computational demand of B2PLYP calculations does not increase its performance significantly, which is similar to the cheaper functional M06.

E_{tor} is much easier to predict and all functionals tested have MUE below chemical accuracy. MAX errors always correspond to **17**, which bent geometry shows increased multiconfigurational character (Table S3 and Section 3.1). Calculated components for $\boldsymbol{\mu}$ are similar among functionals, with the MUE of their magnitude ~ 0.5 D. However, the errors in open-shell flavins are significantly higher for all functionals. For instance, M06-2X shows MUE of 0.25 D for closed-shell and 0.84 D for open-shell flavins. Hence, calculations of flavosemiquinones using DFT for dipole moments and other response properties that depend on electronic polarization by the environment (such as QM/MM simulations in condensed phase) must be seen with caution.

4 | CONCLUSION

A systematic evaluation of approximations in the computation of the molecular electronic structure of isolated flavins was presented here. Multiconfigurational effects are negligible for ground-state properties, except for diradical species in resonance to zwitterionic forms. Including complete basis-set extrapolation and augmented functions in the calculations is necessary for agreement with experimental electron affinities and gas-phase basicities without resorting to error cancellation. The uncertainty expected here for DLPNO-CCSD(T) relative energies is 1.3 mE_h and for MP2 dipole moments it is 0.01 D, suggesting these methods can be used as references for flavin energetic and electrical properties, respectively. Nevertheless, it should be noted that the DLPNO approximation presented high errors for the triples correction to absolute energies, probably due to the delocalized electron distribution in the isoalloxazine ring.

For structural properties, DFT calculations with B3LYP or PBE functionals had similar quality. The popular B3LYP, most often used in previous computational studies of flavins, performs reasonably well for energetic properties but other functionals with similar computational cost are better recommended. For electron affinity calculations, Minnesota hybrid functional M06-2X should be used and for gas-phase basicity, M06 and CAM-B3LYP give the most accurate results. DFT should be carefully used when studying flavosemiquinones and higher level calculations like DLPNO-CCSD(T) are recommended. Pure- and meta-GGA functionals give qualitatively wrong gas-phase basicities and all functionals tested result in large errors for dipole moments of radical flavin forms.

The present analysis of tautomeric equilibria is qualitatively similar to previous studies,[12,14,16] but quantitatively more accurate and embraces a larger and complete set of flavin oxidation and charge states. Tautomeric compositions described here corroborate that nitrogens sites are preferentially protonated, but alternative tautomers are possible and might be explored during catalysis in flavoenzymes.[9] In particular, cationic flavins have unusual protonation at oxygen. Finally, this benchmark study should guide future work in the calculation of redox potentials, pK_a, and other condensed-phase properties for flavins.

ACKNOWLEDGMENT

Funding from Fundação de Amparo à Pesquisa do Estado de São Paulo (FAPESP, scholarship grant 2017/26109-0 to Felipe Curtolo and research grant 2019/21856-7 to Guilherme M. Arantes) is gratefully acknowledged.

DATA AVAILABILITY STATEMENT

The data that support the findings of this study are available from the corresponding author upon reasonable request.

ORCID

Felipe Curtolo https://orcid.org/0000-0002-4459-0968
Guilherme M. Arantes https://orcid.org/0000-0001-5356-7703

REFERENCES

[1] P. F. Heelis, *Chem. Soc. Rev.* **1982**, *11*, 15.
[2] A. M. Edwards, *R. Soc. Chem* **2006**, *6*, 1.
[3] J. M. Christie, L. Blackwood, J. Petersen, S. Sullivan, *Plant Cell Physiol.* **2014**, *56*, 401.
[4] M. A. Vanoni, *Open Biol.* **2021**, *11*, 210010.
[5] E. Romero, J. R. G. Castellanos, G. Gadda, M. W. Fraaije, A. Mattevi, *Chem. Rev.* **2018**, *118*, 1742.
[6] P. F. Fitzpatrick, *Bioorg. Chem.* **2004**, *32*, 125.
[7] F. Curtolo, G. M. Arantes, *J. Chem. Inf. Model.* **2020**, *60*, 6282.
[8] D. Zhong, *Annu. Rev. Phys. Chem.* **2015**, *66*, 691.
[9] H. Unno, S. Yamashita, Y. Ikeda, S. y. Sekiguchi, N. Yoshida, T. Yoshimura, M. Kusunoki, T. Nakayama, T. Nishino, H. Hemmi, *J. Biol. Chem.* **2009**, *284*, 9160.
[10] C. J. Thibodeaux, H.-W. Liu, *Arch. Biochem. Biophys.* **2017**, *632*, 47.
[11] R. K. Kar, A.-F. Miller, M.-A. Mroginski, *WIREs Comput. Mol. Sci.* **2022**, *12*, e1541.
[12] M. Meyer, H. Hartwig, D. Schomburg, *THEOCHEM J. Mol. Struct.* **1996**, *364*, 139.
[13] Y.-L. Zheng, R. L. Ornstein, *J. Am. Chem. Soc.* **1996**, *118*, 9402.
[14] M. Meyer, *THEOCHEM J. Mol. Struct.* **1997**, *417*, 163.
[15] J. Wouters, F. Durant, B. Champagne, J.-M. André, *Int. J. Quantum Chem.* **1997**, *64*, 721.
[16] C. B. Martin, M.-L. Tsao, C. M. Hadad, M. S. Platz, *J. Am. Chem. Soc.* **2002**, *124*, 7226.
[17] S. Salzmann, C. M. Marian, *Chem. Phys. Lett.* **2008**, *463*, 400.
[18] J. Langer, A. Günther, S. Seidenbecher, G. Berden, J. Oomens, O. Dopfer, *ChemPhysChem* **2014**, *15*, 2550.
[19] D. Müller, O. Dopfer, *Phys. Chem. Chem. Phys.* **2020**, *22*, 18328.
[20] D. A. Dixon, D. L. Lindner, B. Branchaud, W. N. Lipscomb, *Biochemistry* **1979**, *18*, 5770.
[21] M. H. Palmer, I. Simpson, R. J. Platenkamp, *J. Mol. Struct.* **1980**, *66*, 243.
[22] L. H. Hall, B. J. Orchard, S. K. Tripathy, *Int. J. Quantum Chem.* **1987**, *31*, 195.
[23] L. H. Hall, B. J. Orchard, S. K. Tripathy, *Int. J. Quantum Chem.* **1987**, *31*, 217.
[24] J. Rodríguez-Otero, E. Martínez-Núñez, A. Peña-Gallego, S. A. Vázquez, *J. Org. Chem.* **2002**, *67*, 6347.
[25] J. D. Walsh, A.-F. Miller, *THEOCHEM J. Mol. Struct.* **2003**, *623*, 185.
[26] Y. Zheng, P. R. Carey, B. A. Palfey, *J. Raman Spectrosc.* **2004**, *35*, 521.

[27] M. Kondo, J. Nappa, K. L. Ronayne, A. L. Stelling, P. J. Tonge, S. R. Meech, *J. Phys. Chem. B* **2006**, *110*, 20107.
[28] S. Bhattacharyya, M. T. Stankovich, D. G. Truhlar, J. Gao, *J. Phys. Chem. A* **2007**, *111*, 5729.
[29] X.-L. Li, Y. Fu, *THEOCHEM J. Mol. Struct.* **2008**, *856*, 112.
[30] M. M. N. Wolf, S. Schumann, R. Gross, T. Domratcheva, R. Diller, *J. Phys. Chem. B* **2008**, *112*, 13424.
[31] M. A. North, S. Bhattacharyya, D. G. Truhlar, *J. Phys. Chem. B* **2010**, *114*, 14907.
[32] R.-K. Zhao, A. Lukacs, A. Haigney, R. Brust, G. M. Greetham, M. Towrie, P. J. Tonge, S. R. Meech, *Phys. Chem. Chem. Phys.* **2011**, *13*, 17642.
[33] M. Kılıç, B. Ensing, *J. Chem. Theory Comput.* **2013**, *9*, 3889.
[34] T. Zhang, K. Papson, R. Ochran, D. P. Ridge, *J. Phys. Chem. A* **2013**, *117*, 11136.
[35] A. Aleksandrov, *J. Comput. Chem.* **2019**, *40*, 2834.
[36] P. Mondal, K. Schwinn, M. Huix-Rotllant, *J. Photochem. Photobiol. A* **2020**, *387*, 112164.
[37] C. Neiss, P. Saalfrank, M. Parac, S. Grimme, *J. Phys. Chem. A* **2003**, *107*, 140.
[38] E. Sikorska, I. V. Khmelinskii, D. R. Worrall, J. Koput, M. Sikorski, *J. Fluoresc.* **2004**, *14*, 57.
[39] E. Sikorska, I. V. Khmelinskii, W. Prukała, S. L. Williams, M. Patel, D. R. Worrall, J. L. Bourdelande, J. Koput, M. Sikorski, *J. Phys. Chem. A* **2004**, *108*, 1501.
[40] E. Sikorska, I. V. Khmelinskii, J. Koput, M. Sikorski, *THEOCHEM J. Mol. Struct.* **2004**, *676*, 155.
[41] E. Sikorska, I. V. Khmelinskii, J. Koput, J. L. Bourdelande, M. Sikorski, *J. Mol. Struct.* **2004**, *697*, 137.
[42] E. Sikorska, J. R. Herance, J. L. Bourdelande, I. V. Khmelinskii, S. L. Williams, D. R. Worrall, G. Nowacka, A. Komasa, M. Sikorski, *J. Photochem. Photobiol. A* **2005**, *170*, 267.
[43] E. Sikorska, I. Khmelinskii, A. Komasa, J. Koput, L. F. V. Ferreira, J. R. Herance, J. L. Bourdelande, S. L. Williams, D. R. Worrall, M. Insińska-Rak, M. Sikorski, *Chem. Phys.* **2005**, *314*, 239.
[44] M. Kowalczyk, E. Sikorska, I. V. Khmelinskii, J. Komasa, M. Insińska-Rak, M. Sikorski, *THEOCHEM J. Mol. Struct.* **2005**, *756*, 47.
[45] M. Insińska-Rak, E. Sikorska, J. L. Bourdelande, I. V. Khmelinskii, W. Prukała, K. Dobek, J. Karolczak, I. F. Machado, L. F. V. Ferreira, A. Komasa, D. R. Worrall, M. Sikorski, *J. Mol. Struct.* **2006**, *783*, 184.
[46] Y.-K. Choe, S. Nagase, K. Nishimoto, *J. Comput. Chem.* **2007**, *28*, 727.
[47] S. Salzmann, J. Tatchen, C. M. Marian, *J. Photochem. Photobiol. A* **2008**, *198*, 221.
[48] M. Wu, L. A. Eriksson, *J. Phys. Chem. A* **2010**, *114*, 10234.
[49] A. Vdovin, A. SlenczkaA, B. Dick, *Chem. Phys.* **2013**, *422*, 195.
[50] B. Karasulu, W. Thiel, *J. Phys. Chem. B* **2015**, *119*, 928.
[51] T. Climent, R. González-Luque, M. Merchán, L. Serrano-Andrés, *J. Phys. Chem. A* **2006**, *110*, 13584.
[52] J. y Hasegawa, S. Bureekaew, H. Nakatsuji, *J. Photochem. Photobiol. A* **2007**, *189*, 205.
[53] S. Salzmann, V.,. V. Martinez-Junza, B. Zorn, S. E. Braslavsky, M. M. Mansurova, C. M. Marian, W. Gärtner, *J. Phys. Chem. A* **2009**, *113*, 9365.
[54] O. Falklöf, B. Durbeej, P. Norman, *J. Phys. Chem. A* **2015**, *119*, 11911.
[55] R. K. Kar, V. A. Borin, Y. Ding, J. Matysik, I. Schapiro, *Photochem. Photobiol.* **2019**, *95*, 662.
[56] F. Abyar, I. Novak, *Spectrochim. Acta A Mol. Biomol. Spectrosc.* **2022**, *264*, 120268.
[57] A. D. Becke, *J. Chem. Phys.* **1993**, *98*, 5648.
[58] P. J. Stephens, F. J. Devlin, C. F. Chabalowski, M. J. Frisch, *J. Phys. Chem.* **1994**, *98*, 11623.
[59] F. Weigend, R. Ahlrichs, *Phys. Chem. Chem. Phys.* **2005**, *7*, 3297.
[60] F. Neese, *WIREs Comput. Mol. Sci.* **2012**, *2*, 73.
[61] F. Neese, *WIREs Comput. Mol. Sci.* **2018**, *8*, e1327.
[62] Curtolo, F.; Arantes, G. M. Lumiflavin molecular structures and energies [Data set]. https://doi.org/10.5281/zenodo.6348046, **2022**.
[63] A. D. Becke, *Phys. Rev. A* **1988**, *38*, 3098.
[64] C. Lee, W. Yang, R. G. Parr, *Phys. Rev. B* **1988**, *37*, 785.
[65] J. P. Perdew, K. Burke, M. Ernzerhof, *Phys. Rev. Lett.* **1996**, *77*, 3865.
[66] Y. Zhao, D. G. Truhlar, *J. Chem. Phys.* **2006**, *125*, 194101.
[67] C. Adamo, V. Barone, V., *J. Chem. Phys.* **1999**, *110*, 6158.
[68] Y. Zhao, D. G. Truhlar, *Theor. Chem. Accounts* **2008**, *120*, 215.
[69] C. Riplinger, P. Pinski, U. Becker, E. F. Valeev, F. Neese, *J. Chem. Phys.* **2016**, *144*, 024109.
[70] R. A. Kendall, T. H. Dunning, R. J. Harrison, *J. Chem. Phys.* **1992**, *96*, 6796.
[71] F. Weigend, A. Köhn, C. Hättig, *J. Chem. Phys.* **2002**, *116*, 3175.
[72] T. Helgaker, P. Jørgensen, J. Olsen, *Molecular Electronic-Structure Theory*, John Wiley & Sons, Ltd, Chichester, England **2000**; Ch.5, p. 142.
[73] T. H. Dunning, *J. Chem. Phys.* **1989**, *90*, 1007.
[74] D. G. Liakos, M. Sparta, M. K. Kesharwani, J. M. L. Martin, F. Neese, *J. Chem. Theory Comput.* **2015**, *11*, 1525.
[75] C. Angeli, R. Cimiraglia, J.-P. Malrieu, *J. Chem. Phys.* **2002**, *117*, 9138.
[76] J. Zheng, X. Xu, D. G. Truhlar, *Theor. Chem. Accounts* **2011**, *128*, 295.
[77] N. C. Handy, A. J. Cohen, *Mol. Phys.* **2001**, *99*, 403.
[78] J. Tao, J. P. Perdew, V. N. Staroverov, G. E. Scuseria, *Phys. Rev. Lett.* **2003**, *91*, 146401.
[79] S. Grimme, J. Antony, S. Ehrlich, H. Krieg, *J. Chem. Phys.* **2010**, *132*, 154104.
[80] S. Grimme, S. Ehrlich, L. Goerigk, *J. Comput. Chem.* **2011**, *32*, 1456.
[81] W.-M. Hoe, A. J. Cohen, N. C. Handy, *Chem. Phys. Lett.* **2001**, *341*, 319.
[82] T. Yanai, D. P. Tew, N. C. Handy, *Chem. Phys. Lett.* **2004**, *393*, 51.
[83] Y. Tawada, T. Tsuneda, S. Yanagisawa, T. Yanai, K. Hirao, *J. Chem. Phys.* **2004**, *120*, 8425.
[84] J.-D. Chai, M. Head-Gordon, *J. Chem. Phys.* **2008**, *128*, 084106.
[85] S. Grimme, *J. Chem. Phys.* **2006**, *124*, 034108.
[86] F. Weigend, *Phys. Chem. Chem. Phys.* **2006**, *8*, 1057.
[87] F. Neese, F. Wennmohs, A. Hansen, U. Becker, *Chem. Phys.* **2009**, *356*, 98.
[88] R. Izsák, F. Neese, *J. Chem. Phys.* **2011**, *135*, 144105.
[89] S. Grimme, *Chem. Eur. J.* **2012**, *18*, 9955.
[90] G. M. Arantes, *J. Phys. Chem. B* **2008**, *112*, 15244.
[91] V. Barone, M. Cossi, *J. Phys. Chem. A* **1998**, *102*, 1995.
[92] A. Karton, J. M. L. Martin, *Theor. Chem. Accounts* **2006**, *115*, 330.
[93] T. Helgaker, W. Klopper, H. Koch, J. Noga, *J. Chem. Phys.* **1997**, *106*, 9639.
[94] D. G. Truhlar, *Chem. Phys. Lett.* **1998**, *294*, 45.
[95] A. Halkier, W. Klopper, T. Helgaker, P. Jørgensen, *J. Chem. Phys.* **1999**, *111*, 4424.
[96] F. Neese, E. F. Valeev, *J. Chem. Theory Comput.* **2011**, *7*, 33.
[97] D. Datta, S. Kossmann, F. Neese, *J. Chem. Phys.* **2016**, *145*, 114101.
[98] J. C. Rienstra-Kiracofe, G. S. Tschumper, H. F. Schaefer, S. Nandi, G. B. Ellison, *Chem. Rev.* **2002**, *102*, 231.
[99] M. Tuckerman, *Statistical Mechanics: Theory and Molecular Simulation*, OUP Oxford, England **2010**; Ch.4, p. 135.
[100] T. J. Lee, P. R. Taylor, *Int. J. Quantum Chem.* **1989**, *36*, 199.
[101] A. Nunes-Alves, G. M. Arantes, *J. Chem. Inf. Model.* **2014**, *54*, 2309.
[102] M. Drosou, C. A. Mitsopoulou, D. A. Pantazis, *J. Chem. Theory Comput.* **2022**, *18*, 6.
[103] R. Norrestam, B. Stensland, *Acta Crystallogr. B* **1972**, *28*, 440.

[104] C. T. W. Moonen, J. Vervoort, F. Mueller, *Biochemistry* **1984**, *23*, 4868.
[105] J. J. P. Stewart, *J. Comput. Chem.* **1989**, *10*, 209.
[106] M. H. Teixeira, G. M. Arantes, *Biochim. Biophys. Acta Bioenerg.* **2019**, *1860*, 541.
[107] M. H. Teixeira, G. M. Arantes, *RSC Adv.* **2019**, *9*, 16892.
[108] M. Kılıç, B. Ensing, *J. Phys. Chem. B* **2019**, *123*, 9751.
[109] G. M. Arantes, *Biochem. J.* **2006**, *399*, 343.
[110] G. M. Arantes, M. C. C. Ribeiro, *J. Chem. Phys.* **2008**, *128*, 114503.

SUPPORTING INFORMATION

Additional supporting information can be found online in the Supporting Information section at the end of this article.

How to cite this article: F. Curtolo, G. M. Arantes, *J. Comput. Chem.* **2022**, 1. https://doi.org/10.1002/jcc.26957